Environmental Pollution 381 (2025) 126623

Contents lists available at ScienceDirect

Environmental Pollution

journal homepage: www.elsevier.com/locate/envpol

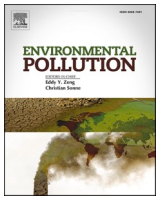

Methane soil gas gradient method for quantifying natural source zone depletion rates at petroleum contaminated sites☆

Iason Verginelli [a,*], Matthew A. Lahvis [b], Parisa Jourabchi [c], George E. DeVaull [b]

[a] Laboratory of Environmental Engineering, Department of Civil Engineering and Computer Science Engineering, University of Rome Tor Vergata, Via del Politecnico 1, 00133, Rome, Italy
[b] Equilon Enterprises LLC doing Business as Shell Oil Products US, Houston, TX, USA
[c] ARIS Environmental Ltd., Vancouver, BC, Canada

ARTICLE INFO

Keywords:
NSZD
Natural attenuation
LNAPL
Petroleum hydrocarbons
Gradient method

ABSTRACT

This study presents a novel method that relies on the methane gradient in soil gas for estimating natural source zone depletion (NSZD) rates of light non-aqueous phase liquids (LNAPL) in the subsurface. Methane generation via methanogenesis at the LNAPL source, followed by methane oxidation in the unsaturated zone, is typically the rate-limiting degradation pathway and can, therefore, serve as a reliable indicator for NSZD rate estimation of bulk LNAPL. Considering that methanogenesis associated with natural soil respiration processes is often negligible, this method can be used to directly convert methane fluxes into NSZD rates. Unlike other methods that focus on O_2, CO_2 or volatile organic compounds (VOCs), this approach is based on an analytical model that incorporates both diffusion and advection-driven transport of methane in soil gas. The application of this model supports the general assumption that diffusion dominates methane transport in the air-connected vadose zone, except in scenarios with high-pressure gradients (e.g., 10 Pa/m) and high soil permeability (e.g., sandy soils), where advection becomes significant relative to diffusion. Additionally, the analysis shows that the overall methane velocity in the aerobic oxidation zone, in most cases, falls within the range of 0.1–1 m/d. By multiplying this velocity by the maximum methane concentration in soil gas and the stoichiometric coefficient of the reference hydrocarbon compound (e.g., 1.14 g_{C8H18}/g_{CH4} for octane), a reliable estimate of the NSZD rate can be derived. When applied to typical soil gas concentrations, this methane gradient method yields NSZD estimates consistent with values reported in the literature, validating its use as a simplified screening approach.

1. Introduction

In recent years, significant advancements have been made in understanding the natural processes responsible for the depletion of light non-aqueous phase liquids (LNAPL) in the subsurface. Initially, the primary mechanism attributed to the natural attenuation of LNAPL was the dissolution of soluble contaminants in groundwater, followed by their biodegradation in the plume (ITRC, 2018). Later, it was shown that methanogenic biodegradation of LNAPL within the source body, followed by methane oxidation in the vadose zone (Pathway 1 in Fig. 1), was the primary driver of source depletion and can account for up to 90–99 % of the overall attenuation of LNAPL in the subsurface (API, 2017; Garg et al., 2017; Lari et al., 2019). In some cases, direct volatilization can also represent a significant component of source depletion, particularly at sites where petroleum LNAPL sources contain a high proportion of volatile hydrocarbons (Guan et al., 2024). This mechanism involves the direct volatilization of LNAPL constituents from the source zone followed by aerobic degradation in the vadose zone (Pathway 2 in Fig. 1). The combination of the processes occurring in both the saturated and unsaturated zone (see Fig. 1) is referred to as natural source zone depletion (NSZD). NSZD occurs at most sites impacted by petroleum hydrocarbons and the measured depletion rates available in the literature range from thousands to tens of thousands of liters per hectare per year (Garg et al., 2017; Kulkarni et al., 2022). To evaluate source zone mass depletion in the saturated zone due to dissolution of LNAPL constituents and attenuation, groundwater samples are typically collected over time at fixed points or varying distances from the source (Newell et al., 2002). In the vadose zone, the main methods for estimating NSZD

☆ This paper has been recommended for acceptance by Hocheol Song.

* Corresponding author.
E-mail address: verginelli@ing.uniroma2.it (I. Verginelli).

https://doi.org/10.1016/j.envpol.2025.126623
Received 11 April 2025; Received in revised form 3 June 2025; Accepted 4 June 2025
Available online 4 June 2025

rates of LNAPL in the vadose zone include CO_2 efflux, temperature gradients and soil gas gradients (API, 2017; ITRC, 2018; ASTM, 2022). These methods provide an estimate of bulk NSZD rates of LNAPL related to both methanogenesis and direct volatilization. Initial approaches relied on soil gas concentration gradients to infer attenuation rates (e.g., Lahvis and Baehr, 1996; Lahvis et al., 1999; Chaplin et al., 2002; Johnson et al., 2006). Later, CO_2 efflux techniques using passive traps or dynamic closed chambers were developed to measure surface fluxes and convert them stoichiometrically into LNAPL degradation rates, based on a representative hydrocarbon (e.g., Sihota et al., 2011; McCoy et al., 2014; Sihota et al., 2018). More recently, temperature gradient methods have been applied to estimate heat fluxes using Fourier's Law, which are then translated into NSZD rates using the heat of reaction from hydrocarbon biodegradation (e.g., Sweeney and Ririe, 2014; Askarani and Sale, 2020).

For the estimation of bulk LNAPL NSZD rates, to account for the natural soil respiration contribution due to natural organic matter decay that can consume oxygen and produce carbon dioxide, the O_2 and CO_2 flux data obtained from the application of these methods should be corrected either by radiocarbon isotopic (14C) analysis or by carrying out measurements in background zones not impacted by LNAPL (API, 2017; ASTM, 2022).

In this work, an alternative gradient method based on methane soil gas profiles is introduced. The main advantage of this new method, compared to the traditional O_2 and CO_2 gradient methods, is that the application of the soil gas gradient method to methane profiles allows a direct estimate of bulk NSZD rates of LNAPL related to methanogenesis without the need for the correction of the rates to account for natural soil respiration. The approach proposed in this work follows a procedure similar to that recently presented by Verginelli et al. (2024) for specific chemicals of concern (COCs), but with a key difference in focus. While Verginelli et al. (2024) concentrated on the direct volatilization of LNAPL constituents and their subsequent biodegradation in the vadose zone (Pathway 2 in Fig. 1), considering only diffusive transport, the present study focuses on the NSZD component associated with methanogenesis and subsequent methane oxidation in the vadose zone (Pathway 1 in Fig. 1), and is based on an analytical solution that accounts for both advection and diffusion. On a long-term basis, it is recognized that diffusion dominates the transport of vapors in the subsurface (McHugh and McAlary, 2009; Hers et al., 2014; USEPA, 2015; Jourabchi and Lin, 2021; Lari et al., 2024). However, in the case of high methane concentrations in the zone within the LNAPL/capillary region, advection could become significant relative to diffusion (Ma et al., 2012; Yao et al., 2015; Cecconi et al., 2023; Lari et al., 2024). In such cases, a soil gas method focused only on diffusion can lead to some underestimation of the NSZD rates. It is also worth noting that the advective fluxes induced by barometric pumping resulting from atmospheric pressure and temperature fluctuations may be relevant near the ground surface in permeable soils, but their influence typically does not extend beyond a depth of 1 m (McHugh and McAlary, 2009; Eklund, 2016; Wang et al., 2023). Consequently, this latter process is not expected to affect soil gas samples collected from probes installed at greater depths. After a brief description of the method, practical tools for a screening of expected NSZD rates based on the maximum methane concentrations detected in the soil gas are provided. To further illustrate the method introduced in this work, an example of application to a case study presented in a recent study (Concawe, 2020) is reported.

2. Methods

2.1. Analytical solution for methane transport in the vadose zone

At steady-state, the reactive transport of methane through the oxidation layer in the aerobic vadose zone can be described by a one-dimensional (1-D) differential equation based on mass balance of advective-diffusive transport and first-order aerobic biodegradation reaction kinetics in a homogeneous soil (Crank, 1979; Van Genuchten and Alves, 1982; DeVaull, 2007; Davis et al., 2009; Verginelli and Baciocchi, 2011):

$$D_e \cdot \frac{d^2C}{dz^2} - u\frac{dC}{dz} - \frac{k_w \cdot \theta_w}{H} \cdot C = 0 \quad (1)$$

where D_e (m^2/s) is the effective diffusion coefficient of methane in the oxidation zone, z (m) is elevation from the bottom of the oxidation zone ($z = 0$), C (g/m^3) is the concentration of methane in soil gas, u (m/s) is the advective velocity in the vadose zone, k_w (s^{-1}) is the first-order aerobic biodegradation reaction rate constant in the aqueous phase, θ_w (m^3/m^3) is the volumetric moisture content of the soil, and H (−) is the dimensionless Henry's Law constant of methane.

As shown in detail in the supplementary information, an analytical solution of eq. (1) can be derived assuming a constant methane concentration, C_{max} (g/m^3), as the lower boundary condition at the bottom of the oxidation zone ($z = 0$) and a negligible flux at the surface ($dC/dz = 0$ and $C = 0$ at $z = L$). Note that the negligible surface flux boundary condition is based on the assumption that methane is completely oxidized within the unsaturated zone, resulting in a negligible concentration gradient and concentration at the soil to atmosphere interface. This assumption is consistent with observations commonly reported in the literature, where vapors are rapidly biodegraded in the vadose zone within very short vertical distances (Lahvis et al., 1999; Hers et al., 2000; Roggemans et al., 2001; Davis et al., 2009; Lahvis et al., 2013;

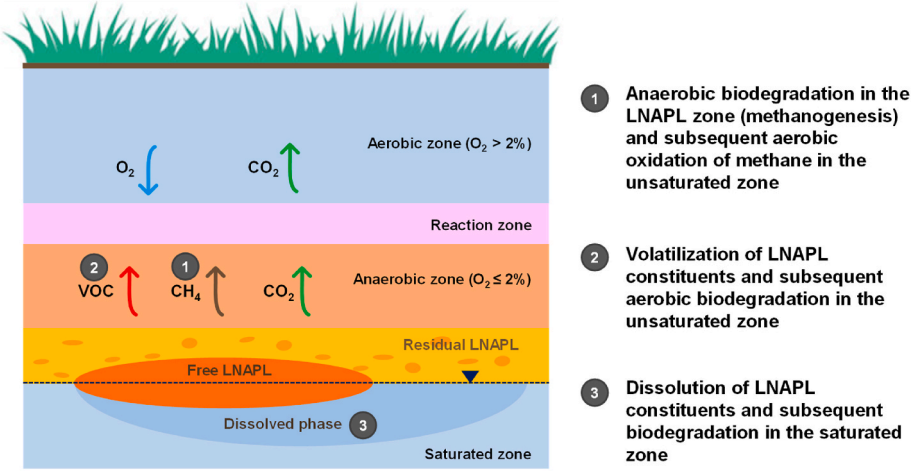

Fig. 1. Conceptual site model of LNAPL attenuation mechanisms in the subsurface.

Hers et al., 2014). Under these assumptions, the following solution that describes the vertical concentration profiles of methane in the aerobic oxidation layer is obtained (see SI for derivation):

$$C(z) = C_{max} \cdot \exp\left(\frac{u \cdot z}{2 \cdot D_e}\right) \cdot [\cosh(\lambda \cdot z) - \beta \cdot sinh(\lambda \cdot z)] \quad (2)$$

with:

$$\beta = \frac{sinh(\lambda \cdot L) + \frac{u}{2 \cdot D_e \cdot \lambda} \cdot \cosh(\lambda \cdot L)}{cosh(\lambda \cdot L) + \frac{u}{2 \cdot D_e \cdot \lambda} sinh(\lambda \cdot L)} \quad (3)$$

$$\lambda = \frac{1}{L_R} + \frac{u}{2D_e} \quad (4)$$

L_R (m) is the advective-diffusive reaction length of methane that can be calculated as follows:

$$L_R = \frac{2D_e}{\sqrt{u^2 + \frac{4D_e \cdot k_w \cdot \theta_w}{H}} - u} \quad (5)$$

As shown in the supplementary information, considering the typical values of D_e, u and k_w for methane in the oxidation zone, $\lambda \cdot L = \frac{L}{L_R} + \frac{u \cdot L}{2D_e} \gg 1$, and consequently for the properties of hyperbolic functions $\beta \approx 1$ (see Fig. S1 in the SI). In such case, eq. (2) can be simplified to:

$$C(z) = C_{max} \cdot exp\left(-\frac{z}{L_R}\right) \quad (6)$$

Note that an analogous solution was previously obtained by Van Genuchten and Alves (1982).

Note that in the case of a diffusion-dominated transport (i.e. negligible u), using the same boundary conditions discussed above, a solution similar to eq. (6) can be obtained (Verginelli et al., 2024), but in this case, the reaction length, $L_{R,diff}$ (m), is defined as (DeVaull, 2007; ITRC, 2014; Verginelli and Baciocchi, 2021):

$$L_{R,diff} = \sqrt{\frac{D_e \cdot H}{\theta_w \cdot k_w}} \quad (7)$$

Similarly, in the case of an advection-dominated transport eq. (6) can still be used but using the following advective reaction length, $L_{R,adv}$ (m):

$$L_{R,adv} = \frac{u \cdot H}{\theta_w \cdot k_w} \quad (8)$$

2.2. Simplified methane gradient method for estimating NSZD rates

The expression for calculating the NSZD rates related to methanogenesis and subsequent oxidation of methane in the unsaturated zone was derived by combining the flux of methane in the in air-connected vadose zone with the analytical solution of the one-dimensional (1-D) steady-state reactive transport model described in the previous section.

In this section, a six-step procedure for applying the soil gas methane gradient method to calculate the NSZD rates is outlined.

2.2.1. Step 1: estimation of the dominant mechanism transport of methane in the oxidation layer

The first step of the procedure involves identifying the dominant transport mechanism of methane in the oxidation layer (i.e., advection-dominated, diffusion-dominated, or a combination of both). To this end, the Peclet Number can be used (Bear and Cheng, 2010; Bear, 2013):

$$Pe = \frac{u \cdot L}{D_e} \quad (9)$$

where Pe (−) is the Peclet number, D_e (m^2/s) is the effective diffusion coefficient of methane in the oxidation zone, u (m/s) is the advective velocity in the vadose zone, and L (m) is the characteristic length.

Based on the estimated Peclet Number, the dominant transport mechanism can be identified as follows (Bear and Cheng, 2010):

$$\begin{cases} Pe \ll 1 & Diffusion - dominated \\ Pe \approx 1 & Diffusion\ and\ Advection \\ Pe \gg 1 & Advection - dominated \end{cases} \quad (10)$$

The relevance of advective flux in the subsurface can be also determined based on the soil gas concentration profile of inert gases such as Ar and N_2 (Amos et al., 2005; Molins et al., 2010). High methanogenesis (i.e., significant generation of methane and carbon dioxide in the source zone) will displace relatively non-reactive atmospheric gases like Ar and N_2 from soil gas (ASTM, 2016), leading to an observed deficit of such gases in the subsurface, with increasing concentrations towards the ground surface and a downward gradient of N_2 and Ar (see Fig. 2a). Considering that the total flux of Ar and N_2 in the subsurface is zero (except for a small amount of nitrogen fixation), the observed downward concentration gradient of Ar and N_2 must be balanced by an upward advective flux (Thorstenson and Pollock, 1989; ASTM, 2016).

As shown by Thorstenson and Pollock (1989), for unidirectional diffusion of CH_4 and CO_2 in stagnant air, the solution of the Stefan-Maxwell equation for an inert gas such as N_2 can be described as:

$$X_{source,N2} = X_{surface,N2} \cdot exp\left(-\frac{u \cdot L_{source}}{D_{e,N2}}\right) \quad (11)$$

where $X_{source,N2}$ (mol/mol) is the molar fraction of N_2 near the LNAPL source zone, $X_{surface,N2}$ (mol/mol) is the molar fraction of N_2 at the ground surface, $D_{e,N2}$ (m^2/s) is the effective diffusion coefficient of N_2 in the subsurface, L_{source} (m) is the depth from ground surface where the greatest N_2 deficit was detected. u (m/s) is the Darcy velocity defined as $u = (R \cdot T/P) \cdot N$ (Thorstenson and Pollock, 1989), where $R \cdot T/P$ is the molar volume (m^3/mol), R (J/mol/K) is the universal gas constant, T (K) is the temperature, P (Pa) is the pressure and N is the molar flux (mol/m^2/s). Note that the same expression can be used for Ar. The molar fraction refers to the proportion of a specific gas (in this case N_2 or Ar) relative to the total number of moles of all gases present in a given volume of air. In this context, it quantifies how much nitrogen (or Ar) is present either at the surface or near the source zone of LNAPL in the subsurface. For example, a N_2 molar fraction of 0.78 at the surface means that 78 % of the moles of gas are nitrogen. The molar fraction of N_2 is a useful way to track changes in gas composition due to subsurface processes like biodegradation, as reductions in nitrogen levels can indicate displacement by other gases such as CH_4 or CO_2.

The argument of the exponential function in eq. (11) can also be expressed in terms of the Peclet number, with $L = L_{source}$. In this context, the Peclet number refers to methane transport, while the expression is derived using N_2 as a conservative tracer, whose diffusive flux is equal and opposite to the advective flux. This leads to:

$$X_{source,N2} = X_{surface,N2} \cdot exp(-Pe) \quad (12)$$

Thus, based on the observed gradient of N_2 (or Ar), the Peclet Number can be calculated from eq. (12) as follows:

$$Pe = -ln\left(\frac{X_{source,N2}}{X_{surface,N2}}\right) \quad (13)$$

2.2.2. Step 2: determination of the reaction length

The reaction length (L_R) of methane in the oxidation layer, can be calculated from eq. (5) using literature values for the diffusion coefficients, the advective velocity and the biodegradation rate constants. Alternatively, the reaction length can be determined from eq. (6) using the soil gas concentrations of methane measured at two depths, C_{upper} and C_{lower}, in the upper and lower control points, respectively, separated by the vertical distance, Δz (m), between the two sampling points (see Fig. 2b):

$$L_R = \frac{\Delta z}{\ln(C_{lower}/C_{upper})} \quad (14)$$

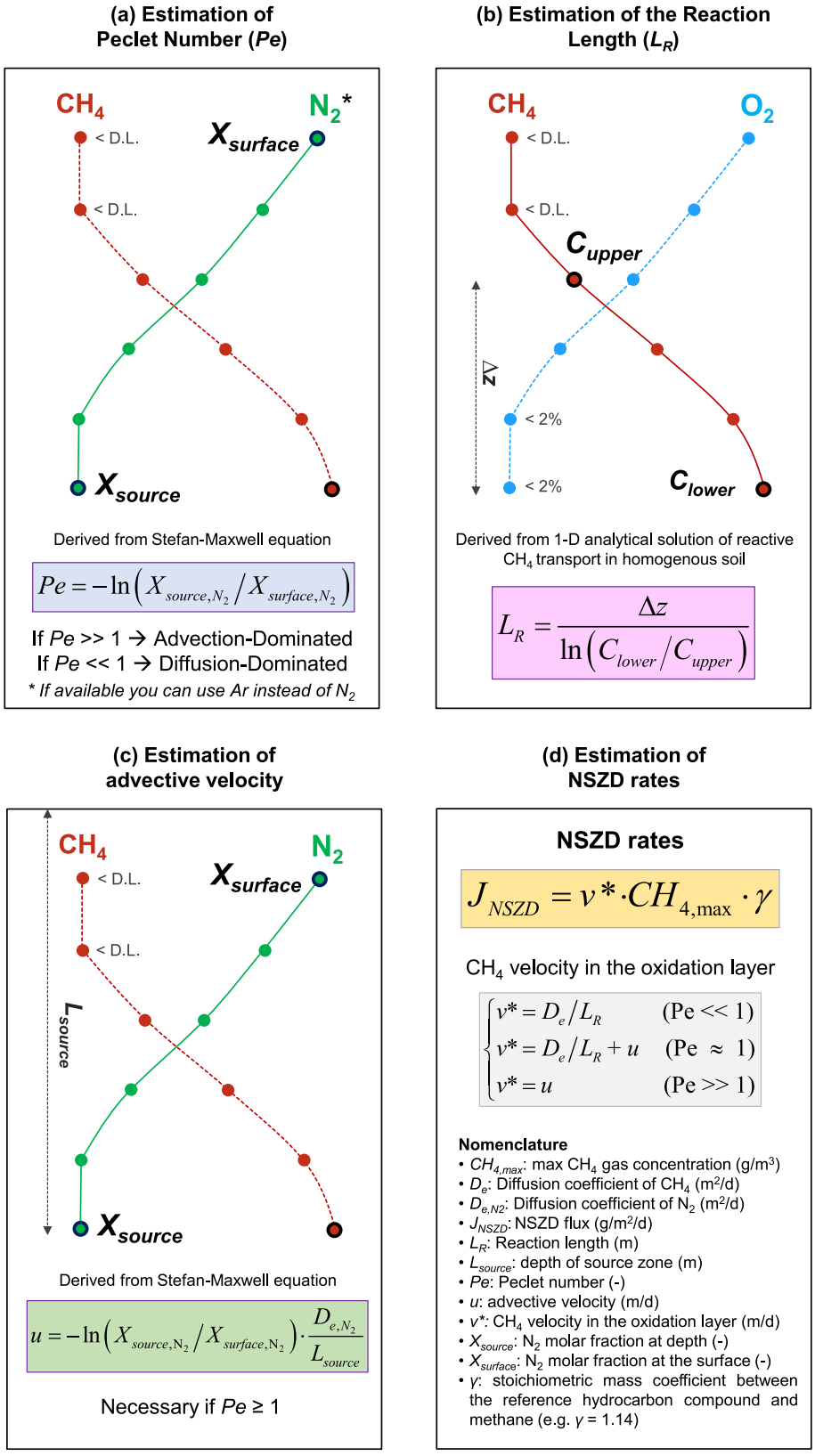

Fig. 2. Methane gradient method proposed in this work. The meaning of the symbols used in the figure can be found in the nomenclature detailed in subfigure d.

The same criteria proposed by Verginelli et al. (2024) to estimate COC-specific NSZD rates can be used to select the control points for methane. In particular, the control points should be selected above the top of the LNAPL source, preferably in the oxidation zone (i.e., where O_2 is higher than 1–2 %), with the lower control point at the bottom of the aerobic zone. Given that the discrete vertical soil gas sampling does not typically include this location at the bottom of the aerobic zone, as a conservative measure, the lower control point (C_{lower}) could generally be

set at the maximum concentration detected at the greatest depth. This leads to a conservative estimate of the fluxes as the longer the Δz, the higher the L_R and thus the lower the estimated NSZD flux. For the upper control point (C_{upper}) the minimum methane concentration above the detection limit (DL) at the top of the reaction zone should be used. It's important to note that if C_{upper} is selected to be at or below the DL, this could potentially lead to an underestimate of the NSZD rate.

2.2.3. Step 3: estimation of the effective diffusion coefficient

The effective diffusion coefficient (D_e) depends on the chemical characteristics of the compound of concern and on the soil type (especially the moisture saturation in the soil). D_e values can be estimated using in-situ soil vapor diffusivity testing with tracer gases as shown by Johnson et al. (1998). When site-specific values are not available, the effective diffusion coefficients can be estimated with the Millington and Quirk (1961) equation:

$$D_e = D_{air} \cdot \frac{\theta_a^{10/3}}{\theta_e^{2}} \tag{15}$$

where D_{air} (m^2/s), is the diffusion coefficient of methane in air, θ_e (m^3/m^3) is the porosity of the soil and θ_a (m^3/m^3) is the air-filled porosity of the soil. Note that in the case of a layered soil, the overall diffusion coefficient in the vadose zone can be calculated by discretizing the system in n layers as suggested by Johnson and Ettinger (1991):

$$D_e = \frac{L}{\sum_i^n \left(\frac{d_i}{D_{e,i}}\right)} \tag{16}$$

where L (m) is the depth of the lower control point below ground surface, d_i (m) is the thickness of the *i-th* layer and $D_{e,i}$ (m^2/s) is the associated diffusion coefficient calculated considering the moisture content and the porosity of this layer.

2.2.4. Step 4: determination of the soil gas velocity

In the case of relevant advection (i.e., $Pe \geq 1$), the soil gas velocity u (m/s) due to advection can be estimated using the following equation (Scanlon et al., 2002):

$$u = \frac{k \cdot k_{rg}}{\mu} \cdot \frac{dp}{dz} \tag{17}$$

where k (m^2) is the effective permeability to soil gas flow, k_{rg} (−) is the relative permeability to gas, μ (kg/m/s) is the dynamic viscosity of soil gas, and dp/dz ($kg/m^2/s^2$, i.e., Pa/m) is the pressure variation.

The relative permeability to gas, k_{rg} (−), can be calculated using the van Genuchten (1980) model (Parker et al., 1987):

$$k_{rg} = S_g^{0.5} \cdot \left(1 - S_L^{1/m}\right)^{2m} \tag{18}$$

where m (−) is the empirical van Genuchten parameter, which depends on the type of soil, and S_g (−) and S_L (−) are the gas and liquid saturation in the soil, respectively.

Alternatively, the soil gas velocity can be estimated from eq. (11) using the N_2 (or Ar) soil gas profiles (see Fig. 2c):

$$u = -ln\left(\frac{X_{source,N2}}{X_{surface,N2}}\right) \cdot \frac{D_{e,N2}}{L_{source}} \tag{19}$$

This latter approach avoids the need to measure small and variable pressure gradients and eliminates the requirement for a permeability estimate.

2.2.5. Step 5: estimation of the methane flux in the oxidation layer

The flux of methane through the oxidation layer in the vadose zone, J_{CH4} ($g/m^2/s$), in the presence of both advection and diffusion, can be calculated as follows:

$$J_{CH4} = -D_e \cdot \frac{dC}{dz} + u \cdot C \tag{20}$$

The concentration gradient (dC/dZ) of the methane in the oxidation layer in the vadose zone can be obtained by differentiating eq. (6) with respect to z:

$$\frac{dC}{dz} = -\frac{C_{max}}{L_R} \cdot exp\left(-\frac{z}{L_R}\right) \tag{21}$$

At the bottom of the oxidation layer ($z = 0$), the concentration gradient is equal to:

$$\left.\frac{dC}{dz}\right|_{z=0} = -\frac{C_{max}}{L_R} \tag{22}$$

Thus, the flux of methane through the oxidation layer, J_{CH4} ($g/m^2/s$), can be obtained by substituting eq. (22) into eq. (20):

$$J_{CH4} = v^* \cdot C_{max} \tag{23}$$

with v^* (m/s) representing the overall methane velocity that depending on the Peclet number can be calculated as (see Fig. 2d):

$$\begin{cases} v^* = \frac{D_e}{L_R} \ (\mathrm{Pe} \ll 1) \\ v^* = \frac{D_e}{L_R} + u \ (\mathrm{Pe} \approx 1) \\ v^* = u \ (\mathrm{Pe} \gg 1) \end{cases} \tag{24}$$

2.2.6. Step 6: estimation of NSZD rates

Based on the estimated flux of methane through the oxidation layer, the NSZD rate of LNAPL can be estimated from the methanogenesis reaction that for a generic reference hydrocarbon can be written as (Verginelli and Baciocchi, 2011):

$$C_nH_m + \left(n - \frac{m}{4}\right)H_2O \rightarrow \left(\frac{n}{2} - \frac{m}{8}\right)CO_2 + \left(\frac{n}{2} + \frac{m}{8}\right)CH_4 \tag{25}$$

Thus, the stoichiometric mass coefficient between the reference hydrocarbon compound and methane can be estimated as follows:

$$\gamma = \frac{MW_{C_nH_m}}{\left(\frac{1}{2}n + \frac{1}{8}m\right)MW_{CH_4}} \tag{26}$$

Considering octane (C_8H_{18}, MW = 114.23 g/mol) as the reference compound (CRC CARE, 2018; ITRC, 2018), the stoichiometric coefficient γ is equal to 1.14 g_{C8H18}/g_{CH4}. Note that the stoichiometric coefficient varies little for a wide range of hydrocarbons (see Table S1).

Appling the stoichiometric coefficient, to the expression derived for the flux of methane through the oxidation layer (eq. (23)), the NSZD rates for LNAPL due to methanogenesis, J_{NSZD} ($g/m^2/s$), can be calculated as follows:

$$J_{NSZD} = v^* \cdot C_{max} \cdot \gamma \tag{27}$$

Assuming octane as the reference hydrocarbon compound (γ = 1.14 gC_8H_{18}/gCH_4), a subsurface temperature of 15 °C and LNAPL density of 0.78 kg/L, the NSZD rates can be easily estimated with the following equations:

$$J_{NSZD}\left[\frac{g}{m^2 \cdot d}\right] = 7.7 \cdot CH_4[\%] \cdot v^*\left[\frac{m}{d}\right] \tag{28}$$

$$J_{NSZD}\left[\frac{gal}{acre \cdot year}\right] = 3,872 \cdot CH_4[\%] \cdot v^*\left[\frac{m}{d}\right] \tag{29}$$

$$J_{NSZD}\left[\frac{L}{ha \cdot year}\right] = 36,170 \cdot CH_4[\%] \cdot v^*\left[\frac{m}{d}\right] \tag{30}$$

Note that, except from environments with high organic loads such as

compost piles, peatlands, or municipal landfills, methanogenesis processes are generally negligible in areas not impacted by LNAPL, with methane concentrations typically undetectable in soil gas (Garg et al., 2017; API, 2017; CRC CARE, 2018; Karimi Askarani et al., 2023). Therefore, the equations presented above are directly applicable to zones affected by LNAPL. In cases where significant methane concentrations are also detected in areas not impacted by LNAPL, it becomes necessary to correct the measured methane values by subtracting the background level, as done in the traditional gradient method (ITRC, 2018).

3. Results and discussion

3.1. Peclet number in the oxidation layer

Fig. 3 shows the Peclet number (*Pe*) in the oxidation layer, calculated using eq. (9), as a function of the pressure gradient (dp/dz) for three types of soil (sand, silt and clay), considering dry (Fig. 3a) or wet conditions (Fig. 3b). The parameters (porosity, soil permeability and Van Genuchten empirical parameter) for the three types of soils were taken from USEPA (2004). For the dry conditions, a soil water saturation (S_w) of 0.2 was considered, while for the wet conditions, which can be considered representative of the behavior in the capillary fringe, a water saturation of 0.8 was assumed. Considering these water contents, the effective diffusion coefficient (D_e) was determined using eq. (15) while the relative permeability was calculated with eq. (18). The first-order biodegradation rate constant of methane in the water phase (k_w) was assumed to be 88 h^{-1}, which corresponds to the median value of the constants obtained by DeVaull et al. (1997) and reported in the ITRC (2014) Petroleum Vapor Intrusion (PVI) guidance. The other input parameters are listed in Table 1. Note that the pressure gradient in the oxidation layer was considered up to a maximum value of 10 Pa/m, as higher values are typically only expected near the LNAPL source zone within the capillary fringe. As shown by Lari et al. (2024), at distances of 10–20 cm from the source, the pressure gradient values in the unsaturated soil quickly drop below 10 Pa/m. For example, in a crude oil spill site near Bemidji, Molins et al. (2010) detected maximum pressure gradients in the unsaturated zone of 0.07 Pa/m. In the case study presented in the API NSZD guidance (API, 2017), which was characterized by high methane concentrations, the pressure gradients reached up to 10–20 Pa/m (0.1–0.3 inches of water at a depth of 11 feet).

Table 1
Input Parameters (unless otherwise noted in figures).

Parameter	Symbol	Units	Value	Notes
Soil porosity	θ_e	m^3/m^3	0.375	Sand (USEPA, 2004)
			0.489	Silt (USEPA, 2004)
			0.459	Clay (USEPA, 2004)
Soil permeability	k	m^2	$9.90\bullet10^{-12}$	Sand (USEPA, 2004)
			$6.79\bullet10^{-13}$	Silt (USEPA, 2004)
			$2.30\bullet10^{-13}$	Clay (USEPA, 2004)
Empirical Van Genuchten parameter	m	–	0.31	Sand (USEPA, 2004)
			0.60	Silt (USEPA, 2004)
			0.80	Clay (USEPA, 2004)
Soil water saturation	S_w	–	0.2	Dry conditions
			0.8	Wet conditions
Relative permeability (dry conditions)	k_{rg}	–	0.89	Sand (see eq. (18))
			0.82	Silt (see eq. (18))
			0.71	Clay (see eq. (18))
Relative permeability (wet conditions)	k_{rg}	–	0.29	Sand (see eq. (18))
			0.11	Silt (see eq. (18))
			0.05	Clay (see eq. (18))
Pressure gradient	dp/dz	Pa/m	0.01–10	Typical values expected in the subsurface
Dynamic viscosity of soil gas	μ	kg/m/s	$1.8x10^{-6}$	–
Air diffusion coefficient of CH_4	D_{air}	m^2/h	0.07	API (2012)
Dimensionless Henry Constant of CH_4	H	–	29	API (2012)
Biodegradation rate constant of CH_4	k_w	h^{-1}	88	Median value reported in ITRC (2014)
Stoichiometric HC to CH_4 mass ratio	γ	g/g	1.14	See eq. (26)

From Fig. 3a it can be observed that for dry soil conditions ($S_w = 0.2$), for pressure gradients less than 1 Pa/m, $Pe \ll 1$ for all types of soil indicating a diffusion-dominated transport. For pressure gradients higher than 1 Pa/m, in the case of sandy soils, $Pe > 1$ indicating the establishment of an advection-dominated transport. For silt and clay the Peclet number is always less than 1 even at relatively high-pressure gradients (i.e., 10 Pa/m), suggesting that the assumption of a diffusion-dominated transport can be considered always valid. A similar behavior is expected under wet conditions ($S_w = 0.8$) although in this case the establishment of an advection-dominated transport for sandy

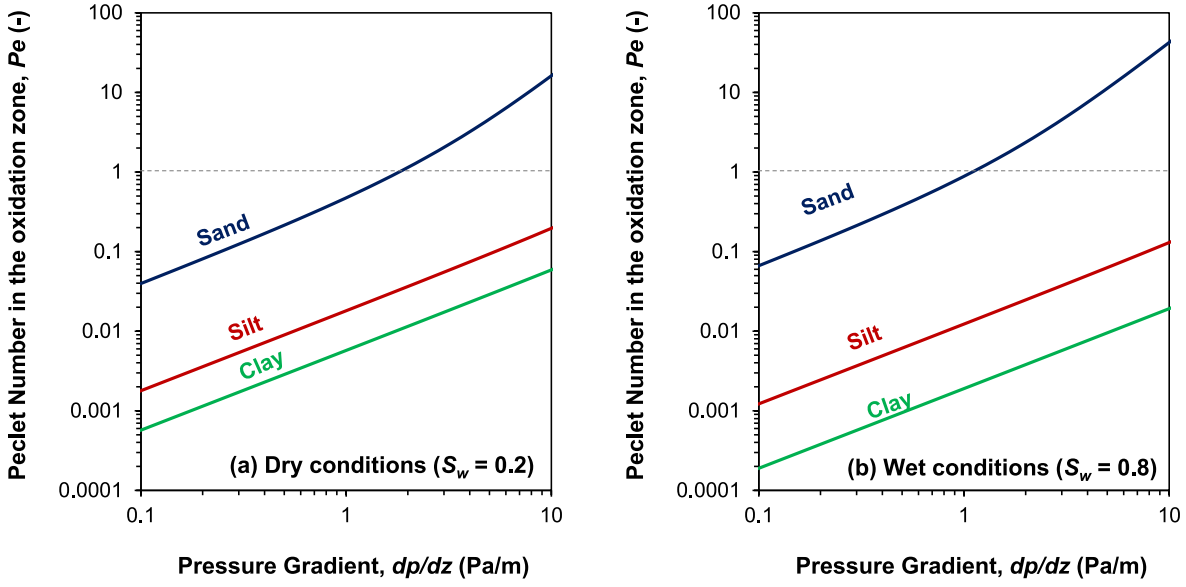

Fig. 3. Peclet Number (*Pe*) in the oxidation layer calculated as a function of the pressure gradient (dp/dz) in the oxidation layer for three types of soil (sand, silt and clay) under (a) dry conditions ($S_w = 0.2$) or (b) wet conditions ($S_w = 0.8$).

soils can be expected at slightly lower pressure gradients (see Fig. 3b) compared to dry soils (see Fig. 3a). These findings align with Lari et al. (2024), who used a sophisticated numerical model to conclude that advection is significant only in a thin zone close to the LNAPL source.

3.2. Reaction length of methane in the case of advection and diffusion

Fig. 4 shows the reaction length of methane (L_R), calculated using eq. (5), as a function of the Peclet Number considering dry (Fig. 4a) or wet conditions (Fig. 4b). The input parameters used for these estimates are the same as those discussed in the previous section (see Table 1).

For dry conditions ($S_w = 0.2$), from Fig. 4a it can be observed that for $Pe < 1$, the reaction length is almost constant at approximately 0.2 m. This value corresponds to the reaction length calculated with eq. (7) assuming a diffusion-dominated transport and is consistent with the values reported for methane in the ITRC (2014) guidance. For $Pe \gg 1$, the reaction length can reach values up to almost 1 m. This suggests that in such cases if the LNAPL source is shallow (e.g., <3 m) the oxidation of methane can be not completed with consequent methane emissions into the atmosphere. A similar behavior is expected under wet conditions ($S_w = 0.8$). However, in this case, the reaction length is expected to remain in the order of a few centimeters (see Fig. 4b), as the vapors move very slowly due to the high-water content, ensuring an attenuation of methane concentration within very short vertical distances.

3.3. Velocity of methane in the subsurface in the presence of advection and diffusion

Fig. 5 shows the expected velocity of methane in soil gas within the oxidation layer (v^*), calculated with eq. (24b) as a function of the Peclet number under (a) dry or (b) wet conditions. Each figure also illustrates the contribution to the overall methane velocity (represented by continuous lines) from both diffusion and advection (represented by dotted lines). The input parameters used for these estimates are the same as those discussed in the previous sections (see Table 1).

From these figures, it can be observed that for $Pe < 1$ (i.e., diffusion-dominated transport), the methane velocity in the subsurface is almost constant at approximately 1 m/d for dry conditions and 0.2 m/d for wet conditions. As shown in the figures, these velocities are almost entirely attributed to diffusion (see red dotted lines). For $Pe \gg 1$, in the case of dry conditions velocities higher than 5 m/d can be expected. This increase in velocity is attributed to the advective component (see green dotted lines), while the diffusion velocity for high-pressure gradients decreases due to the increase in the reaction length (see Fig. 4), leading to a reduction in the (D_e/L_R) ratio. Also for wet soils a slightly increase in the methane velocity is expected for $Pe \gg 1$ although the overall velocity values are always expected to keep below 1 m/d.

Based on these results, two important aspects can be highlighted. First, as already discussed in previous section, in nearly all cases, the contribution of advection to the migration of methane in the oxidation zone is negligible. Second, for screening purposes, a methane velocity in the subsurface in the range of 0.1–1 m/d could be used as reasonable values that cover a wide range of scenarios.

3.4. Screening of NSZD rates

Fig. 6 presents the NSZD rates calculated using the developed method (see eq. (27)) as a function of the maximum methane concentrations detected in soil gas (expressed in percentage) and the overall methane velocity in the subsurface considering both advection and diffusion ($v^* = u + D_e/L_R$) that according to previous estimates was varied between 0.1 and 10 m/d. Note that to convert the concentration of methane expressed in percentage to g/m^3, a reference temperature of 15 °C and a pressure of 1 atm were considered. The conversion of methane fluxes to LNAPL NSZD rates was carried out assuming octane (C_8H_{18}) as a reference compound with a stoichiometric coefficient of 1.14 g_{C8H18}/g_{CH4} (see section 2.2.6). Also note that in the figure, the NSZD rates were calculated up to a maximum methane concentration of 10 %. For higher concentrations the model is still applicable but tends to be less accurate, as the use of Fick's Law can introduce increasing bias. For example, as reported in the ASTM (2016) standard guidance, for methane mole fraction concentrations around 0.20, the application of Fick's Law can result in an error of approximately 25 %, which is likely within the spatio-temporal variability of NSZD rates typically encountered at petroleum release sites. To achieve more reliable estimates at higher concentrations, more complex models than Fick's Law (e.g., Stefan-Maxwell) may be preferred (Thorstenson and Pollock, 1989; Amos and Mayer, 2006).

Based on the analysis reported in the previous section, under dry conditions a velocity of 1 m/d can be used for screening purposes (e.g., see Fig. 5a). Using this velocity in Fig. 6, it can be observed that the range of NSZD rates expected for methane concentrations varying from

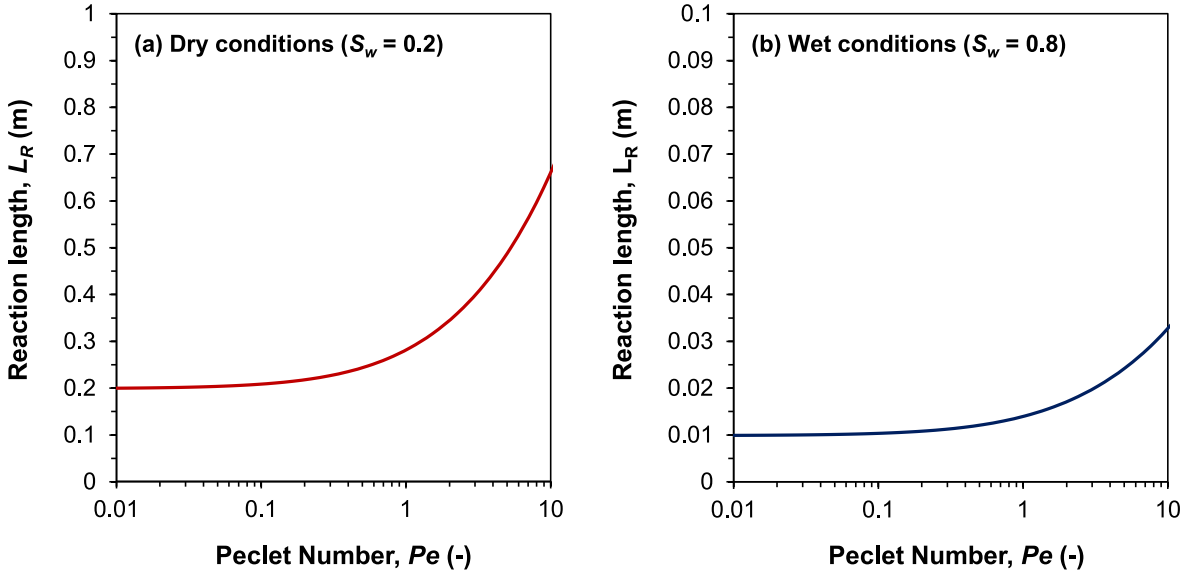

Fig. 4. Reaction length of methane (L_R) calculated with eq. (5) as a function of the Peclet number (Pe) considering (a) dry conditions ($S_w = 0.2$) or (b) wet conditions ($S_w = 0.8$).

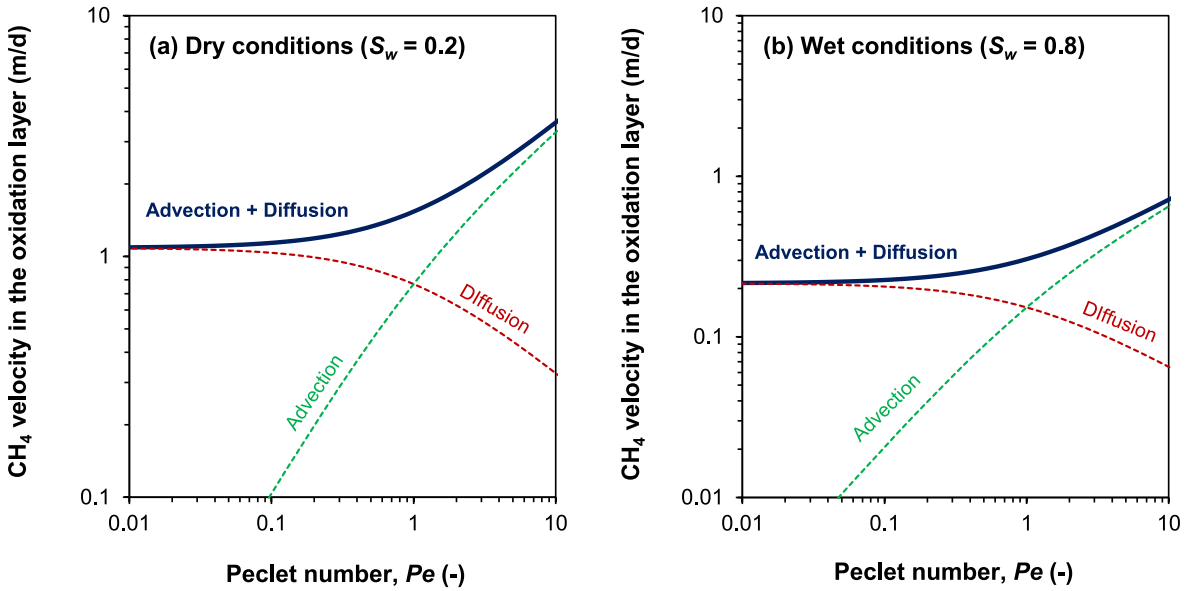

Fig. 5. Velocity of methane expected in the oxidation layer in the unsaturated zone (v^*) as a function of the Peclet number (*Pe*) under (a) dry conditions ($S_w = 0.2$) or (b) wet conditions ($S_w = 0.8$). The dotted lines represent the contribution to the overall methane velocity ascribed to diffusion and advection.

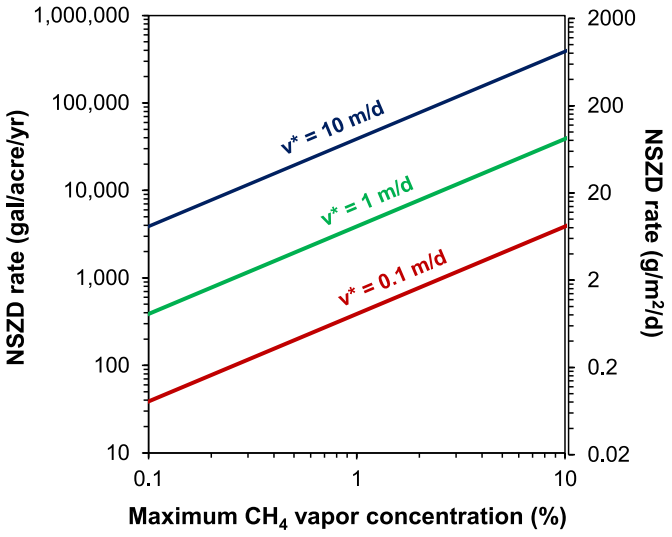

Fig. 6. NSZD rates calculated as a function of methane vapor concentration and overall methane velocity ($v^* = D_e/L_R + v$). Note that 1 g/m^2/d = 501 gal/acre/yr assuming a LNAPL density of 0.78 kg/L. For methane, 1 % ≈ 6.78 g/m^3 (@ 15 °C and 1 atm).

0.1 % to 10 % is approximately 400 to 40,000 gallons per acre per year. This range aligns with the typical NSZD rates observed in the field. For instance, Garg et al. (2017) and Kulkarni et al. (2022), who reviewed NSZD rates measured at various sites, reported ranges of 300 to 7700 gallons per acre per year and 300 to 2720 gallons per acre per year, respectively. This qualitative example confirms the validity of the proposed method and suggests that methanogenesis is one of the dominant attenuation processes contributing to the overall NSZD rates. Thus, for screening purposes, the maximum methane concentration detected in soil gas probes or monitoring wells can be used to estimate the expected NSZD rates.

It is important to highlight that, as reported by Guan et al. (2024), when methane concentrations are low (e.g., $CH_4 < 0.1$ %), the volatilization of individual LNAPL constituents from the source zone, followed by their biodegradation in the subsurface, becomes a significant contributor to overall source depletion. In such scenarios, NSZD rates for a range of hydrocarbons resulting from the direct volatilization of VOCs and subsequent aerobic biodegradation can be estimated using the methodology proposed by Verginelli et al. (2024).

3.5. Example of application of the screening method

The screening gradient method illustrated in the previous section was applied to a case study presented in a recent report by Concawe (2020) and Smith et al. (2021). This case study refers to a dismissed site formerly occupied by a retail fueling station. The site was characterized by the presence of shallow residual LNAPL near former underground storage tanks and dispensers. At this site, three methods were applied to estimate NSZD rates: the soil gas concentration gradient method based on the O_2 and CO_2 vertical profiles detected in monitoring wells and soil gas probes, the biogenic heat method and the CO_2 efflux method using passive traps. For additional details on the site and the methods applied, readers are directed to the report of Concawe (2020).

Based on the maximum methane concentration detected in the soil gas probes and monitoring wells, the simplified screening method presented in the previous section was applied (see eq. (30)). This method was applied to the area of the site characterized by gasoline contamination, considering only the monitoring points with a concentration of methane of at least 0.1 %. For the application of the method, a methane velocity of 1 m/d was considered. The methane fluxes were converted to NSZD rates considering a stoichiometric mass coefficient of 1.14 g/g and a LNAPL density of 0.78 kg/L. The outcome of this analysis is reported in Table 2. The estimated NSZD rates in the different points were in the range of 3255 to 39,787 L/ha/yr, with a mean value of 17,087 L/ha/yr.

Table 3 presents a comparison of the NSZD rates calculated using this method with those reported in Concawe (2020), which utilized the O_2 and CO_2 gradient method and CO_2 traps. It can be observed that the simplified approach presented in this work yields data close to the range observed with CO_2 passive traps, while the O_2/CO_2 gradient method significantly underestimates the attenuation rates (on average by a factor of 50).

As indicated by the authors (Concawe, 2020), the underestimation of NSZD rates resulting from the traditional O_2/CO_2 gradient method can be attributed to the limited vertical resolution of the probes, which were unable to capture soil gas composition changes near the base of the vadose zone, where vertical soil gas concentration gradients are highest. Additionally, another possible reason for this underestimation is the

Table 2
Estimation of NSZD rates based on maximum methane concentrations. The data refer to the case study presented by Smith et al. (2021) and Concawe (2020).

ID Point (Date)	Monitoring point	CH_4 max (%)	NSZD rate – CH_4 method (L/ha/yr)
SV3 (Jan 2018)	SGS probe	0.5	18,085
SV4 (Jan 2018)	SGS probe	0.45	16,277
S-5(June 2017)	GW well	0.4	14,468
S-6 (June 2017)	GW well	0.3	10,851
S-10 (June 2017)	GW well	0.3	10,851
S-16 (June 2017)	GW well	0.6	21,702
S-17 (June 2017)	GW well	0.3	10,851
S-6 (Oct 2017)	GW well	0.3	10,851
S-10 (Oct 2017)	GW well	0.4	14,468
S-15 (Oct 2017)	GW well	0.2	7234
S-16 (Oct 2017)	GW well	0.5	18,085
S-17 (Oct 2017)	GW well	0.4	14,468
S-5 (Jan 2018)	GW well	1.1	39,787
S-6 (Jan 2018)	GW well	0.7	25,319
S-10 (Jan 2018)	GW well	1	36,170
S-15 (Jan 2018)	GW well	0.7	25,319
S-16 (Jan 2018)	GW well	0.7	25,319
S-17 (Jan 2018)	GW well	0.8	28,936
S-5 (Apr 2018)	GW well	0.13	4702
S-6 (Apr 2018)	GW well	0.11	3979
S-10 (Apr 2018)	GW well	0.09	3255
S-15 (Apr 2018)	GW well	0.13	4702
S-16 (Apr 2018)	GW well	0.7	25,319
S-17 (Apr 2018)	GW well	0.8	28,936
S-16 (Jul 2018)	GW well	0.2	7234
Arithmetic Mean		**0.1**	**17,087**
Min		**1.1**	**3255**
Max		**0.47**	**39,787**
5th percentile		**0.11**	**4123**
25th percentile		**0.3**	**10,851**
50th percentile (Median)		**0.4**	**14,468**
75th percentile		**0.7**	**25,319**
95th percentile		**0.96**	**34,723**

Table 3
Comparison of estimated NSZD rates based on the methane gradient method with the other methods applied in Concawe (2020).

Method	Range: Min-Max (L/ha/yr)	Mean (L/ha/yr)	Reference
O_2/CO_2 gradient method (vapor probes)	85–490	260	Concawe (2020)
O_2/CO_2 gradient method (monitoring wells)	52 - 2700	1100	Concawe (2020)
CO_2 passive traps	17,000–130,000	54,000	Concawe (2020)
CH_4 gradient method	3255–39,787	17,087	This Work

approximation of O_2 and CO_2 gradients to linear profiles, which, as shown by Verginelli and Baciocchi (2021), can lead to an underestimation of NSZD rates.

This underestimation is significantly reduced when using the methane gradient method, although the NSZD rates are still lower (on average by a factor of 3) than those obtained using the CO_2 efflux method. These underestimations can be partly attributed to the input parameters used in the method (e.g., the methane velocity in the oxidation layer) as well as to the limited vertical resolution, which may hinder the identification of the maximum methane concentration. Additionally, part of the underestimation may result from the contribution of direct volatilization of individual LNAPL constituents from the source zone, followed by their subsequent biodegradation in the subsurface (Guan et al., 2024; Verginelli et al., 2024).

This illustrative example however further confirms that the method presented in this work can help to easily identify the expected NSZD rates, providing conservative results (i.e., lower NSZD rates) compared to the actual rates.

4. Conclusions

The method presented in this study offers a practical way to estimate NSZD rates at hydrocarbon-contaminated sites with significant subsurface methane concentrations (>0.1 %). Specifically, the NSZD rates can be calculated based on the methane velocities in the subsurface and the maximum methane concentrations detected in soil gas probes or the headspace of piezometers. As shown in the study, methane velocities of 0.1–1 m/d in the oxidation zone can be assumed for a broad range of conditions where diffusion is the main transport process. Indeed, except for high-pressure gradients (i.e., 10 Pa/m) and highly permeable soils (i.e., sand), advection can be considered negligible compared to diffusion. Based on this evidence, simple relationships have been proposed to estimate NSZD rates solely from the expected methane velocity and the maximum methane concentrations detected in the subsurface.

When compared with literature values, these estimates are well-aligned, confirming the reliability of this method. Additionally, applying this method to a case study (Concawe, 2020) has shown that it could refine estimates compared to the traditional gradient method based on O_2 and CO_2 profiles, which could have underestimated NSZD rates due to the limited vertical resolution of soil gas probes or the assumption of linear concentration gradients.

When applying the model, its limitations related to the simplifying assumptions must be considered. Firstly, the model assumes the existence of an aerobic zone and a complete oxidation of methane in the air-connected soil above the LNAPL source. Although this is typically observed at sites, it needs to be verified on a case-by-case basis, especially in the case of paved surfaces, shallow LNAPL sources or large buildings that can limit the replenishment of oxygen in the subsurface (Knight and Davis, 2013; Verginelli and Baciocchi, 2014; Verginelli et al., 2016). Furthermore, the presented method assumes that methanogenesis is the dominant attenuation process. In cases where methane concentrations are below 0.1 % and VOC concentrations exceed 100 ppm, this assumption may no longer be valid, as volatilization of LNAPL constituents and their biodegradation in the unsaturated zone can contribute significantly to overall NSZD rates, as shown by Verginelli et al. (2024) and Guan et al. (2024).

Another aspect to consider is the application of the diffusive model based on Fick's law, which could lead to approximations of fluxes for methane concentrations above 10–20 %. In such cases, more complex models may be preferred (Thorstenson and Pollock, 1989; Amos and Mayer, 2006). Finally, it should be noted that the developed model can be used to describe methane behavior in the aerobic vadose zone with air-connected pores. In the saturated zone and at the soil to groundwater interface, during methanogenesis processes, groundwater can become supersaturated, and gas bubble formation (i.e., ebullition) may occur episodically (Amos and Mayer, 2006; Sihota et al., 2013; Soucy and Mumford, 2017). In these areas, diffusion is significantly reduced (approaching values typical of diffusion in water), and advection becomes the dominant transport mechanism.

Bearing in mind these aspects, the developed method can serve as an effective and simple additional line of evidence compared to those typically gathered in NSZD studies.

CRediT authorship contribution statement

Iason Verginelli: Writing – original draft, Methodology, Investigation, Formal analysis, Data curation, Conceptualization. **Matthew A. Lahvis:** Writing – review & editing, Supervision, Methodology. **Parisa Jourabchi:** Writing – review & editing, Supervision, Methodology. **George E. DeVaull:** Writing – review & editing, Supervision, Methodology.

Declaration of competing interest

The authors declare that they have no known competing financial interests or personal relationships that could have appeared to influence the work reported in this paper.

Appendix A. Supplementary data

Supplementary data to this article can be found online at https://doi.org/10.1016/j.envpol.2025.126623.

Data availability

Data will be made available on request.

References

Amos, R.T., Mayer, K.U., Bekins, B.A., Delin, G.N., Williams, R.L., 2005. Use of dissolved and vapor-phase gases to investigate methanogenic degradation of petroleum hydrocarbon contamination in the subsurface. Water Resour. Res. 41 (2), W02001. https://doi.org/10.1029/2004WR003433.

Amos, R.T., Mayer, K.U., 2006. Investigating ebullition in a sand column using dissolved gas analysis and reactive transport modeling. Environ. Sci. Technol. 40 (17), 5361–5367. https://doi.org/10.1021/es0602501.

API, 2012. BioVapor, A 1-D Vapor Intrusion Model with Oxygen-Limited Aerobic Biodegradation. American Petroleum Institute. http://www.api.org. (Accessed 1 June 2025).

API, 2017. Quantification of Vapor phase-related Natural Source Zone Depletion Processes. American Petroleum Institute. Publication No. 4784. http://www.api.org. (Accessed 1 June 2025).

Askarani, K.K., Sale, T.C., 2020. Thermal estimation of natural source zone depletion rates without background correction. Water Res 169, 115245. https://doi.org/10.1016/j.watres.2019.115245.

ASTM, 2016. Standard Guide for Evaluating Potential Hazard as a Result of Methane in the Vadose Zone. ASTM, p. 16. E2993.

ASTM, 2022. Standard Guide for Estimating Natural Attenuation Rates for Non-aqueous Phase Liquids in the Subsurface. ASTM, p. E3361, 22.

Bear, J., Cheng, A.H.D., 2010. Modeling Groundwater Flow and Contaminant Transport, vol. 23. Springer, Dordrecht.

Bear, J., 2013. Dynamics of fluids in porous media. Courier Corporation. North Chelmsford, MA.

Cecconi, A., Verginelli, I., Barrio-Parra, F., De Miguel, E., Baciocchi, R., 2023. Influence of advection on the soil gas radon deficit technique for the quantification of LNAPL. Sci. Total Environ. 875, 162619. https://doi.org/10.1016/j.scitotenv.2023.162619.

Chaplin, B.P., Delin, G.N., Baker, R.J., Lahvis, M.A., 2002. Long-term evolution of biodegradation and volatilization rates in a crude oil-contaminated aquifer. Bioremediation 6, 237–255. https://doi.org/10.1080/10889860290777594.

Concawe, 2020. Detailed evaluation of natural source zone depletion at a paved former petrol station. Concawe Report 13/20. Concawe, Brussels. https://www.concawe.eu/wp-content/uploads/Rpt_20-13.pdf. (Accessed 1 June 2025).

Crank, J., 1979. The Mathematics of Diffusion. Oxford University Press, Oxford.

CRC CARE, 2018. Technical measurement guidance for LNAPL natural source zone depletion. CRC CARE Technical Report No. 44. CRC for Contamination Assessment and Remediation of the Environment. Newcastle, Australia. https://crccare.com/wp-content/uploads/2022/12/CRCCARETechnicalreport44_TechnicalmeasurementguidanceforLNAPLnaturalsourcezonedepletion.pdf. (Accessed 1 June 2025).

Davis, G.B., Patterson, B.M., Trefry, M.G., 2009. Evidence for instantaneous oxygen-limited biodegradation of petroleum hydrocarbon vapors in the subsurface. Ground water monit. Rem 29 (1), 126–137. https://doi.org/10.1111/j.1745-6592.2008.01221.x.

DeVaull, G.E., Ettinger, R.A., Salanitro, J.P., Gustafson, J.B., 1997. Benzene, toluene, ethylbenzene, and xylenes (BTEX) degradation in vadose zone soils during vapor transport: first-order rate constants. Ground Water Publishing Co. No. CONF-971116-).

DeVaull, G.E., 2007. Indoor vapor intrusion with oxygen-limited biodegradation for a subsurface gasoline source. Environ. Sci. Technol. 41 (9), 3241–3248. https://doi.org/10.1021/es061618t.

Eklund, B., 2016. Effect of environmental variables on vapor transport. In: Proceedings of the 26th Annual International Conference on Soil, Water, Energy, and Air. San Diego, CA.

Garg, S., Newell, C.J., Kulkarni, P.R., King, D.C., Adamson, D.T., Renno, M.I., Sale, T., 2017. Overview of natural source zone depletion: processes, controlling factors, and composition change. Ground Water Monit. Remed. 37 (3), 62–81. https://doi.org/10.1111/gwmr.12219.

Guan, J., Li, C., Yu, W., Wei, G., Kang, R., Pang, H., McHugh, T., Ma, J., 2024. Impacts of LNAPL types on mechanisms and rate of natural source zone depletion. Environ. Pollut. 356, 124380. https://doi.org/10.1016/j.envpol.2024.124380.

Hers, I., Atwater, J., Li, L., Zapf-Gilje, R., 2000. Evaluation of vadose zone biodegradation of BTX vapours. J. Contam. Hydrol. 46 (3–4), 233–264. https://doi.org/10.1016/S0169-7722(00)00135-2.

Hers, I., Jourabchi, P., Lahvis, M.A., Dahlen, P., Luo, H., Johnson, P., DeVaull, G.E., Mayer, K.U., 2014. Evaluation of seasonal factors on petroleum hydrocarbon vapor biodegradation and intrusion potential in a cold climate. Ground Water Monit. Remed. 34 (4), 60–78. https://doi.org/10.1111/gwmr.12085.

ITRC, 2014. Petroleum Vapor Intrusion: Fundamentals of Screening, Investigation, and Management. Interstate Technology & Regulatory Council, Vapor Intrusion Team, Washington, D.C. https://projects.itrcweb.org/PetroleumVI-Guidance/Content/Resources/PVIPDF.pdf. (Accessed 1 June 2025).

ITRC, 2018. Light non-aqueous phase liquids (LNAPL) document update, LNAPL-3. Interstate Technology & Regulatory Council, LNAPL Update Team. Washington, D.C. https://lnapl-3.itrcweb.org/. (Accessed 1 June 2025).

Johnson, P.C., Bruce, C., Johnson, R.L., Kemblowski, M.W., 1998. In situ measurement of effective vapor-phase porous media diffusion coefficients. Environ. Sci. Technol. 32 (21), 3405–3409. https://doi.org/10.1021/es980186q.

Johnson, P.C., Ettinger, R.A., 1991. Heuristic model for predicting the intrusion rate of contaminant vapors into buildings. Environ. Sci. Technol. 25 (8), 1445–1452. https://doi.org/10.1021/es00020a013.

Johnson, P., Lundegard, P., Liu, Z., 2006. Source zone natural attenuation at petroleum hydrocarbon spill sites—I: site-specific assessment approach. Ground Water Monit. Remed. 26 (4), 82–92. https://doi.org/10.1111/j.1745-6592.2006.00114.x.

Jourabchi, P., Lin, G.K., 2021. Modeling vapor migration for estimating the time to reach steady state conditions. Ground Water Monit. Remed. 41 (1), 25–32. https://doi.org/10.1111/gwmr.12480.

Karimi Askarani, K., Sale, T., Palaia, T., 2023. Natural source zone depletion of petroleum hydrocarbon NAPL. In: García-Rincón, J., Gatsios, E., Lenhard, R.J., Atekwana, E.A., Naidu, R. (Eds.), Advances in the Characterisation and Remediation of Sites Contaminated with Petroleum Hydrocarbons, Environmental Contamination Remediation and Management, vol. 5. Springer, Cham, pp. 113–138. https://doi.org/10.1007/978-3-031-34447-3_5.

Knight, J.H., Davis, G.B., 2013. A conservative vapour intrusion screening model of oxygen-limited hydrocarbon vapour biodegradation accounting for building footprint size. J. Contam. Hydrol. 155, 46–54. https://doi.org/10.1016/j.jconhyd.2013.09.005.

Kulkarni, P.R., Walker, K.L., Newell, C.J., Askarani, K.K., Li, Y., McHugh, T.E., 2022. Natural source zone depletion (NSZD) insights from over 15 years of research and measurements: a multi-site study. Water Res. 225, 119170. https://doi.org/10.1016/j.watres.2022.119170.

Lahvis, M.A., Baehr, A.L., 1996. Estimation of rates of aerobic hydrocarbon biodegradation by simulation of gas transport in the unsaturated zone. Water Resour. Res. 32 (7), 2231–2249. https://doi.org/10.1029/96WR00805.

Lahvis, M.A., Baehr, A.L., Baker, R.J., 1999. Quantification of aerobic biodegradation and volatilization rates of gasoline hydrocarbons near the water table under natural attenuation conditions. Water Resour. Res. 35 (3), 753–765. https://doi.org/10.1029/1998WR900087.

Lahvis, M.A., Hers, I., Davis, R.V., Wright, J., DeVaull, G.E., 2013. Vapor intrusion screening at petroleum UST sites. Ground water monit. Rem 33 (2), 53–67. https://doi.org/10.1111/gwmr.12005.

Lari, K.S., Davis, G.B., Rayner, J.L., Bastow, T.P., Puzon, G.J., 2019. Natural source zone depletion of LNAPL: a critical review supporting modelling approaches. Water Res. 157, 630–646. https://doi.org/10.1016/j.watres.2019.04.001.

Lari, K.S., Davis, G.B., Rayner, J.L., Bastow, T.P., 2024. Advective and diffusive gas phase transport in vadose zones: importance for defining vapour risks and natural source zone depletion of petroleum hydrocarbons. Water Res. 255, 121455. https://doi.org/10.1016/j.watres.2024.121455.

Ma, J., Rixey, W.G., DeVaull, G.E., Stafford, B.P., Alvarez, P.J., 2012. Methane bioattenuation and implications for explosion risk reduction along the groundwater to soil surface pathway above a plume of dissolved ethanol. Environ. Sci. Technol. 46 (11), 6013–6019. https://doi.org/10.1021/es300715f.

McHugh, T.E., McAlary, T., 2009. Important physical processes for vapor intrusion: a literature review. In: Proceedings of AWMA Vapor Intrusion Conference. San Diego, CA.

McCoy, K., Zimbron, J., Sale, T., Lyverse, M., 2014. Measurement of natural losses of LNAPL using CO_2 traps. Ground Water 53 (4), 658–667. https://doi.org/10.1111/gwat.12240.

Millington, R.J., Quirk, J.P., 1961. Permeability of porous solids. Trans. Faraday Soc. 57, 1200–1207. https://doi.org/10.1039/TF9615701200.

Molins, S., Mayer, K.U., Amos, R.T., Bekins, B.A., 2010. Vadose zone attenuation of organic compounds at a crude oil spill site—Interactions between biogeochemical reactions and multicomponent gas transport. J. Contam. Hydrol. 112 (1–4), 15–29. https://doi.org/10.1016/j.jconhyd.2009.09.002.

Newell, C.J., Rifai, H.S., Wilson, J.T., Connor, J.A., Aziz, J.A., Suarez, M.P., 2002. Calculation and use of first-order rate constants for monitored natural attenuation studies. In: EPA/540/S-02/500. US Environmental Protection Agency National Risk Management Research Laboratory, Cincinnati, OH, USA. https://nepis.epa.gov/Exe/ZyPURL.cgi?Dockey=10004674.TXT. (Accessed 1 June 2025).

Parker, J.C., Lenhard, R.J., Kuppusamy, T., 1987. A parametric model for constitutive properties governing multiphase flow in porous media. Water Resour. Res. 23 (4), 618–624. https://doi.org/10.1029/WR023i004p00618.

Roggemans, S., Bruce, C.L., Johnson, P.C., Johnson, R.L., 2001. Vadose zone natural attenuation of hydrocarbon vapors: an emperical assessment of soil gas vertical profile data. In: API Soil and Groundwater Research Bulletin, pp. 1–12. https://www.api.org/~/media/files/ehs/clean_water/bulletins/15_bull.pdf. (Accessed 1 June 2025).

Scanlon, B.R., Nicot, J.P., Massmann, J.W., 2002. Soil gas movement in unsaturated systems. Soil Phys. Companion 389, 297–341. https://doi.org/10.1201/9781420041651.ch8.

Sihota, N., Singurindy, O., Mayer, K.U., 2011. CO_2-Efflux measurements for evaluating source zone natural attenuation rates in a petroleum hydrocarbon contaminated aquifer. Environ. Sci. Technol. 45 (2), 482–488. https://doi.org/10.1021/es1032585.

Sihota, N.J., Mayer, K.U., Toso, M.A., Atwater, J.F., 2013. Methane emissions and contaminant degradation rates at sites affected by accidental releases of denatured fuel-grade ethanol. J. Contam. Hydrol. 151, 1–15. https://doi.org/10.1016/j.jconhyd.2013.03.008.

Sihota, N., McAlexander, B., Lyverse, M., Mayer, K.U., 2018. Multi-year CO_2 efflux measurements for assessing natural source zone depletion at a large hydrocarbon-impacted site. J. Contam. Hydrol. 219, 50–60. https://doi.org/10.1016/j.jconhyd.2018.10.007.

Smith, J.J., Benede, E., Beuthe, B., Marti, M., Lopez, A.S., Koons, B.W., Kirkman, A.J., Barreales, L.A., Grosjean, T., Hjort, M., 2021. A comparison of three methods to assess natural source zone depletion at paved fuel retail sites. Q. J. Eng. Geol. Hydrogeol. 54 (4). https://doi.org/10.1144/qjegh2021-005 qjegh2021-005.

Soucy, N.C., Mumford, K.G., 2017. Bubble-facilitated VOC transport from LNAPL smear zones and its potential effect on vapor intrusion. Environ. Sci. Technol. 51 (5), 2795–2802. https://doi.org/10.1021/acs.est.6b06061.

Sweeney, R.E., Ririe, G.T., 2014. Temperature as a tool to evaluate aerobic biodegradation in hydrocarbon contaminated soil. Ground Water Monit. Remed. 34 (3), 41–50. https://doi.org/10.1111/gwmr.12064.

Thorstenson, D.C., Pollock, D.W., 1989. Gas transport in unsaturated zones: multicomponent systems and the adequacy of Fick's laws. Water Resour. Res. 25 (3), 477–507. https://doi.org/10.1029/WR025i003p00477.

USEPA, 2004. User's guide for evaluating subsurface vapor intrusion into buildings. Prepared by Environmental Quality Management for USEPA Office of Emergency and Remedial Response. https://www.epa.gov/sites/default/files/2015-11/documents/2004_0222_3phase_users_guide.pdf. (Accessed 1 June 2025).

USEPA, 2015. Technical guide for addressing petroleum vapor intrusion at leaking underground storage tank sites. EPA 510-R-15-001, Office of Underground Storage Tanks. Washington, D.C. http://www.epa.gov/oust/cat/pvi/pvi-guide-final-6-10-15.pdf. (Accessed 1 June 2025).

Van Genuchten, M.T., 1980. A closed-form equation for predicting the hydraulic conductivity of unsaturated soils. Soil Sci. Soc. Am. J. 44 (5), 892–898. https://doi.org/10.2136/sssaj1980.03615995004400050002x.

Van Genuchten, M.T., Alves, W.J., 1982. Analytical Solutions of the One-Dimensional Convective-Dispersive Solute Transport Equation. U.S. Department of Agriculture, p. 151. Technical Bulletin No. 1661. https://www.ars.usda.gov/arsuserfiles/20361500/pdf_pubs/P0753.pdf. (Accessed 1 June 2025).

Verginelli, I., Baciocchi, R., 2011. Modeling of vapor intrusion from hydrocarbon-contaminated sources accounting for aerobic and anaerobic biodegradation. J. Contam. Hydrol. 126 (3–4), 167–180. https://doi.org/10.1016/j.jconhyd.2011.08.010.

Verginelli, I., Baciocchi, R., 2014. Vapor intrusion screening model for the evaluation of risk-based vertical exclusion distances at petroleum contaminated sites. Environ. Sci. Technol. 48 (22), 13263–13272. https://doi.org/10.1021/es503723g.

Verginelli, I., Yao, Y., Wang, Y., Ma, J., Suuberg, E.M., 2016. Estimating the oxygenated zone beneath building foundations for petroleum vapor intrusion assessment. J. Hazard. Mater. 312, 84–96. https://doi.org/10.1016/j.jhazmat.2016.03.037.

Verginelli, I., Baciocchi, R., 2021. Refinement of the gradient method for the estimation of natural source zone depletion at petroleum contaminated sites. J. Contam. Hydrol. 241, 103807. https://doi.org/10.1016/j.jconhyd.2021.103807.

Verginelli, I., Lahvis, M.A., Jourabchi, P., DeVaull, G.E., 2024. Soil gas gradient method for estimating natural source zone depletion rates of LNAPL and specific chemicals of concern. Water Res. 267, 122559. https://doi.org/10.1016/j.watres.2024.122559.

Wang, Q., Xie, H., Peng, Y., Mohammad, A., Singh, D.N., 2023. VOCs emission from a final landfill cover system induced by ground surface air temperature and barometric pressure fluctuation. Environ. Pollut. 336, 122391. https://doi.org/10.1016/j.envpol.2023.122391.

Yao, Y., Wu, Y., Wang, Y., Verginelli, I., Zeng, T., Suuberg, E.M., Jiang, L., Wen, Y., Ma, J., 2015. A petroleum vapor intrusion model involving upward advective soil gas flow due to methane generation. Environ. Sci. Technol. 49 (19), 11577–11585. https://doi.org/10.1021/acs.est.5b01314.